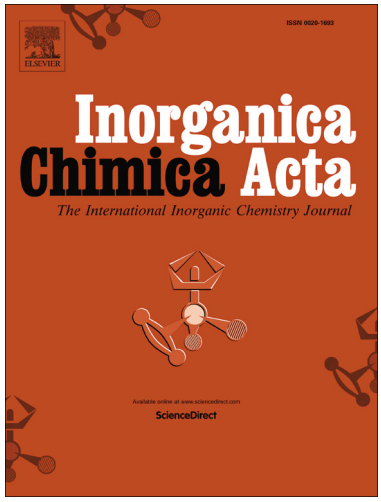

A benzothiazole-based chemosensor for significant fluorescent turn-on and ratiometric detection of Al^{3+} and its application in cell imaging

Shuang Zeng, Shi-Jie Li, Xue-Jiao Sun, Ming-Qiang Li, Zhi-Yong Xing, Jin-Long Li

PII: S0020-1693(18)31376-8
DOI: https://doi.org/10.1016/j.ica.2018.11.042
Reference: ICA 18657

To appear in: *Inorganica Chimica Acta*

Received Date: 1 September 2018
Revised Date: 23 November 2018
Accepted Date: 26 November 2018

Please cite this article as: S. Zeng, S-J. Li, X-J. Sun, M-Q. Li, Z-Y. Xing, J-L. Li, A benzothiazole-based chemosensor for significant fluorescent turn-on and ratiometric detection of Al^{3+} and its application in cell imaging, *Inorganica Chimica Acta* (2018), doi: https://doi.org/10.1016/j.ica.2018.11.042

A benzothiazole-based chemosensor for significant fluorescent turn-on and ratiometric detection of Al^{3+} and its application in cell imaging

Shuang Zeng [a,1], Shi-Jie Li [b,1], Xue-Jiao Sun [a], Ming-Qiang Li [a], Zhi-Yong Xing [a,*], Jin-Long Li [c]

[a] Department of Applied Chemistry, College of Science, Northeast Agricultural University, Harbin 150030, PR China

[b] College of Life Science, Northeast Agricultural University, Harbin 150030, PR China

[c] School of Chemistry and Chemical Engineering, Qiqihar University, Qiqihar 161006, PR China

* Corresponding author at: Department of Applied Chemistry, College of Science, Northeast Agricultural University, Harbin 150030, PR China

E-mail addresses: zyxing@neau.edu.cn, Tel: +86 451 5519 1810, Fax: +86 451 5519 0317

[1] These authors contributed equally to this work and should be considered co-first authors.

Abstract: Chemosensor **Z** including benzothiazole fluorophore was synthesized and characterized with NMR and HRMS spectroscopic techniques. **Z** exhibited fluorescence turn-on and ratiometric absorbance detection of Al^{3+} ions based on the combination mechanism of CHEF and ESIPT processes. Moreover, the stiochiometry between **Z** and Al^{3+} were determined 2:1 through job's plot and HRMS, and the limit of detection was determined as 8.47 nM which was qualified in the detection of Al^{3+} in drinking water. Especially, **Z** was achieved in fast identification the existence of Al^{3+} by filter paper, and cell imaging in human stromal cell (HSC).

Key Words: benzothiazole; Al^{3+}; ratiometric detection; filter paper; cells HSC

1. Introduction

Aluminum, one of the most abundant metal elements in the earth's crust, is closely associated with our daily life [1-4]. However, abnormal concentrations of Al^{3+} in the human body is detrimental to the health of human owing to it can cause a number of diseases, such as Alzheimer's disease, Parkinson's disease, liver damages, amyotrophic lateral sclerosis, anemia, and hemochromatosis [5-8]. Moreover, high concentration of Al^{3+} has obvious reverse effects on the growth of seeds and roots [9, 10] and can kill fish in acidified water [11]. So, it is a challenge to find an efficient method for qualitative and quantitative analysis of Al^{3+} in complex environments and vivo as well.

Recently, many researchers have paid more attention on the development of fluorescent probe, but the detection and quantification of Al^{3+} is always a challenging work owing to the strong hydration of Al^{3+} in aqueous media, thus leading to its weak coordination ability compared with transition metals. Although a lot of fluorescent probe were successfully developed in the detection of Al^{3+}, there are still some deficiencies, such as weak selectivity, poor solubility in water and muti-step synthetic methods, which limit their further application. Therefore, advancement in the synthesis of sensitive, selective and water solubility of Al^{3+} probes is still in high demands. 2-(2'-Hydroxyphenyl) benzothiazole (HBT) as a fluorophore have been widely used in construction chemosensors in the recent years because of its distinguished properties in photophysical and photochemical fields mainly embodied in its facile structural modification, dual emission via the excited state intramolecular proton transfer (ESIPT), and excellent photo stability [12-14]. Furthermore, Al^{3+}, known as a hard acid, prefers a hard-base coordination sphere containing N and O as the binding sites [15-17], in order to improve the binding ability with Al^{3+},

as show in Scheme 1, a novel HBT-based fluorescent chemosensor **Z**, affording N and O as binding sites, had been synthesized by condensation reaction of compound **2** with 4-Hydroxybenzohydrazide. The chemosensor **Z** itself had weak light yellow fluorescence, due to the C=N isomerization and possible two-way ESIPT process (Scheme 2). After the chemosensor **Z** coordinate with Al^{3+}, the C=N isomerization and ESIPT processes were both inhibited, hence leading to the chelation induced enhanced fluorescence (CHEF). The exciting results showed that chemosensor **Z** exhibited highly selectivity to Al^{3+} with a significant fluorescence enhancement and ratiometric absorption detection in DMF-H_2O (1/9, v/v, pH = 7.4, 0.01 M HEPES). Moreover, chemosensor **Z** was achieved in the detection of Al^{3+} in real water samples, test paper, CIE diagram and cell imaging in human stromal cell (HSC).

2. Experimental

2.1. Materials and instruments

Unless otherwise specified, all the solvents and reagents (analytical or spectroscopic grade) were obtained commercially and used without further purification. ^{1}H NMR spectra and ^{13}C NMR spectra were recorded on a Bruck AV-600 spectrometer. Chemical shifts (δ) are reported in ppm using DMSO-d_6 as the solvent. Absorption spectra were recorded on a Pgeneral TU-1901 UV–vis spectrometer at 25 ℃. Fluorescence measurements were measured on a Perkin Elmer LS55 fluorescence spectrometer. Mass spectra were measured on a Waters Xevo UPLC/G2-SQ Tof MS spectrometer. The melting point was measured on a Beijing XT4-100X microscopic melting point apparatus. The pH measurements were recorded using a model PHS-3C meter (Shanghai, China). Cell images were collected using a laser confocal microscope (Leica, TCS SP2 AOBS).

2.2. Synthesis

2.2.1 Synthesis of compound **1**-**2**

According to reported methods, compound 2-(benzo[d]thiazol-2-yl) phenol (**1**), which was synthesized through condensation reaction of 2-aminobenzenethiol with 2-hydroxy-5-methylbenzaldehyde [18], was used for the synthesis of 3-(benzo[d]thiazol-2-yl)-2-hydroxybenzaldehyde (**2)** through Duff reaction [19]. Sensor **Z** was prepared through condensation reaction between compound **2** and 4-hydroxybenzohydrazide (Scheme 1).

2.2.2 Synthesis of Sensor **Z**

The compound **2** (99.5 mg, 0.37 mmol) and 4-Hydroxybenzohydrazide (58 mg, 0.38 mmol) were dissolved in ethanol (20 mL), and then the reaction mixture was refluxed 4 h (monitored by TLC). After completion of reaction, the mixture was cooled to room temperature. The solid was filtered, washed 5 times with ethanol and dried under vacuum to get the light yellow product **Z** (122 mg, yield 82%). ^{1}H NMR (600 MHz, DMSO-d6) (Fig. S1) δ (ppm) 13.42 (s, 1H), 12.18 (s, 1H), 10.23 (s, 1H), 8.66 (s, 1H), 8.22 (s, 1H), 8.17 (d, J = 8.0 Hz, 1H), 8.09 (d, J = 8.0 Hz, 1H), 7.87 (d, J = 8.5 Hz, 2H), 7.60 – 7.52 (m, 2H), 7.47 (td, J = 7.7, 1.0 Hz, 1H), 6.91 (d, J = 8.7 Hz, 2H), 2.40 (s, 3H). ^{13}C NMR (151 MHz, DMSO-d_6) (Fig. S2) δ (ppm) 163.03, 162.45, 161.00, 153.88, 151.26, 147.08, 134.84, 133.01, 130.05, 129.74, 128.47, 126.34, 124.98, 122.80, 122.18, 121.91, 119.42, 119.39, 115.09, 19.83. HRMS (m/z) (TOF MS ES$^-$) (Fig. S3): calcd for $C_{22}H_{16}N_3O_3S$: 402.0912 [M-H]$^-$, found: 402.0903.

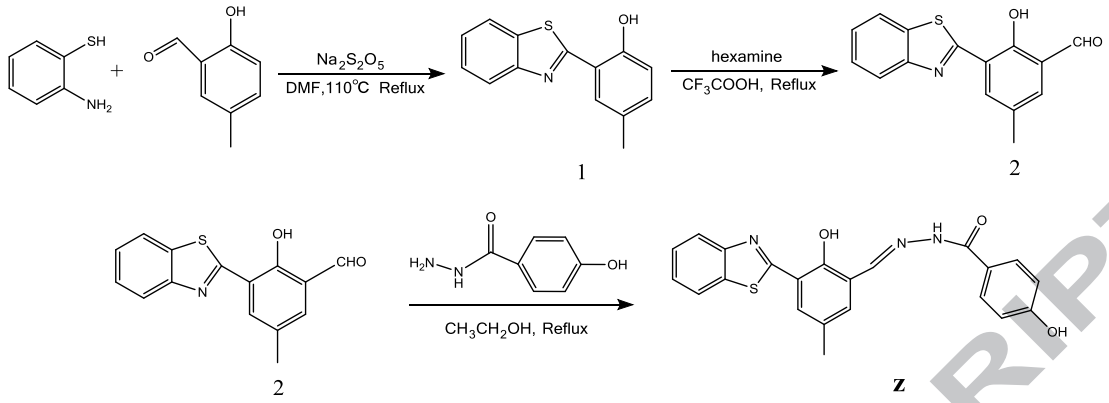

Scheme 1. Synthesis of sensor **Z**.

2.3. General information

The stock solution of **Z** (0.1 mM) was prepared in DMF, then diluted with HEPES buffer (10 mM, pH 7.4)/DMF (1/9, v/v) to 10 μM for the measurement of UV-vis absorption and fluorescence spectra, respectively. The stock solutions (10 mM) of the cationic salts (Na^+, K^+, Mg^{2+}, Ca^{2+}, Ba^{2+}, Cr^{3+}, Mn^{2+}, Fe^{2+}, Fe^{3+}, Co^{2+}, Ni^{2+}, Cu^{2+}, Ag^+, Zn^{2+}, Cd^{2+}, Hg^{2+}, Al^{3+} and Pb^{2+}) were prepared with ultrapure water, respectively. The excitation was set at 350 nm for the measurement of fluorescence, and slit widths of the excitation and emission were 10 nm and 10 nm, respectively.

2.4. Preparation of [**Z**-Al^{3+}]

The compound **Z** (10 mg, 0.025 mmol) and $Al(NO_3)_3 \cdot 9H_2O$ (9.4 mg, 0.025 mmol) were dissolved in ethanol (10 mL). Then the mixture was refluxed for 2 h under stirring. The solution turned to deep yellow and cooled to the temperature. The **Z**-Al^{3+} complexes were obtained by removing the solvent under reduced pressure. Yield: 86%, color: yellow solid.

2.5. Cell culture and staining

The human stromal cell (HSC) purchased from ATCC (CRL-4003) was routinely cultured in 1:1 mixture of DMEM medium and F-12 medium supplemented with 10% heat-inactivated FBS, 100 U/mL penicillin, 100 μg/mL streptomycin, and 1mM sodium pyruvate at 37 ℃, 5% CO_2 for

maintained. After plant HSC into 35 mm plates at concentration of 5×10^4 cells/cm^2, the media without FBS or antibiotic, was used for culture cells and chemical treatment. These cells were incubated 1 hour with different amounts of Al^{3+} (0, 5 and 50 μM). Then fibroblast cells of every group were washed with PBS 3 times and were fixed by using a standard paraformaldehyde fixation protocol. After fixation, fibroblast cells were rinsed with 4:6 mixture solution of DMF and water and then stained by incubating for 2 hours with **Z** (1×10^{-4} M). Lastly, the cells were mounted in standard mounting media and imaged by laser confocal microscope. The excitation wavelength and an emission wavelength were set at 405 nm and 490 nm, respectively.

3. Results and Discussion

The chemosensor **Z** was synthesized and characterized by ^{1}H NMR, ^{13}C NMR and HRMS spectrum analysis depicted in scheme 1.

3.1. UV-vis and Fluorescence spectra characteristics for ions

The fluorescence spectral responses of **Z** toward different metal ions (Mn^{2+}, Na^+, Ni^{2+}, Ca^{2+}, K^+,Mg^{2+}, Ba^{2+}, Cr^{3+}, Fe^{2+}, Fe^{3+}, Co^{2+}, Cu^{2+}, Zn^{2+}, Ag^+, Hg^{2+}, Cd^{2+}, Al^{3+} and Pb^{2+}) were investigated to ascertain the selectivity of **Z** in DMF/H_2O(1/9, v/v, pH = 7.4, 0.01 M HEPES). As shown in Fig. 1a, probe **Z** displayed a weak fluorescence-emission (λ_{em} = 506 nm) which may be due to the two aspects as followed. Firstly, the isomerization of C=N moiety, reported by some researchers [20-22], was the dominant decay process. Secondly, the possible two-way ESIPT process of **Z** could lead to fluorescence quenching caused by the nonradiative decay of the excited state (Scheme 2) [23-25]. Interestingly only Al^{3+} caused a drastic enhancement in the emission intensity of **Z** with a prominent peak at 496 nm, which induced by the inhibition of C=N

isomerization and ESIPT processes upon the coordination of Al^{3+} with **Z**, hence causing chelation induced enhanced fluorescence (CHEF) [23, 24]. Moreover, the solution of **Z** displayed a visible color change from light yellow to brilliant cyan, which easily detected by naked-eye under UV light of 365 nm. As for UV-visible absorbance spectrum, the free **Z** showed two absorption bands at 300 and 375 nm in DMF/H_2O (1/9, v/v, pH = 7.4, 0.01 M HEPES) solution. However, upon addition of Al^{3+}, the absorption band at 375 nm disappeared and new bands at 325 nm, 340 nm, 425 nm were observed, indicated the formation of complexation between **Z** and Al^{3+} (Fig. 1b). These results indicated the possibility of probe **Z** for the identification of Al^{3+} with good selectivity.

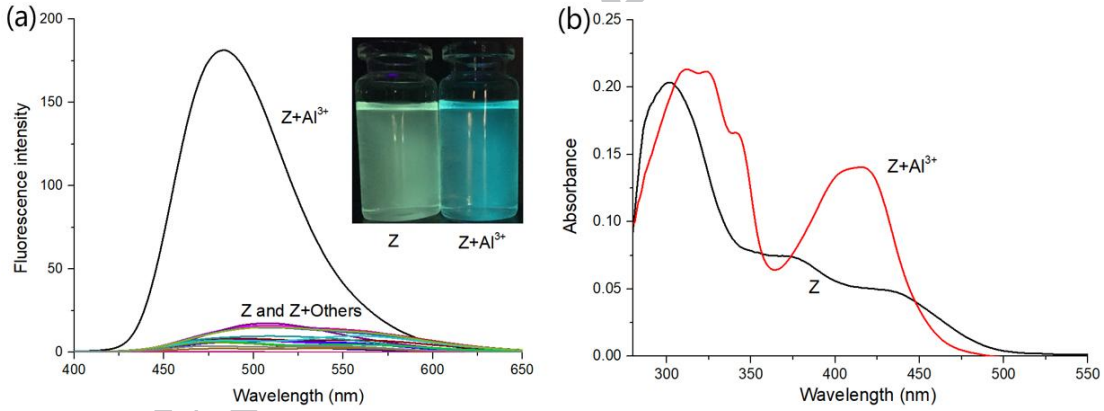

Fig. 1. (a) Fluorescence emission spectra (λ_{ex}=350 nm) of **Z** (10 μM) in the presence of 5 equiv. of various metal ions in DMF-H_2O(1/9, v/v, pH = 7.4, 0.01 M HEPES). Inset: The color changes of **Z** (10 μM) in the presence of Al^{3+} ions (5 equiv.) in DMF-H_2O (1/9, v/v, containing 0.01 M HEPES, pH = 7.4) under UV light of 365 nm. (b) Absorption spectra of **Z** (10 μM) recorded without and with 5.0 equiv. Al^{3+} in DMF-H_2O(1/9, v/v, pH = 7.4, 0.01 M HEPES).

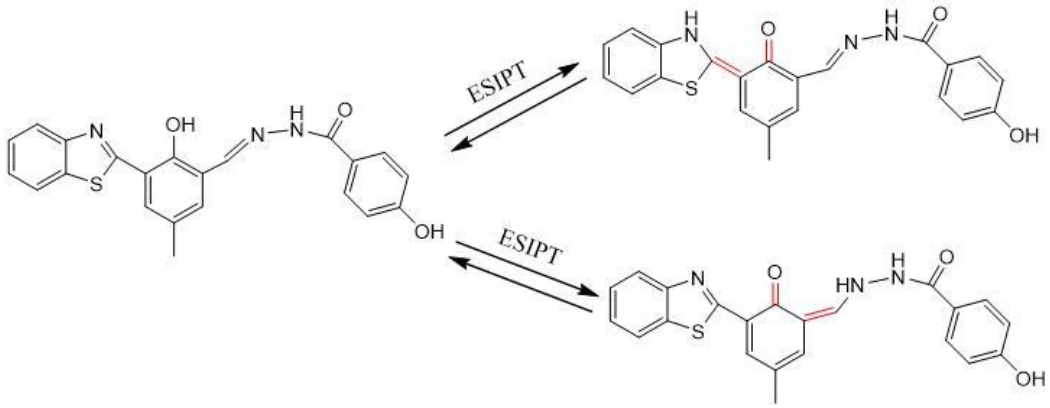

Scheme 2. Probable two-way ESIPT of sensor **Z**.

Subsequently, the experiments including fluorescence and UV–vis titration were measured in order to evaluate the sensing ability of **Z** to Al^{3+}, respectively (Fig. 2). Upon the addition of Al^{3+} (0–1.0 equiv.) to the solution of **Z**, the emission intensity at 496 nm increased gradually and then almost reached a platform when the addition of Al^{3+} was 5μM (0.5 equiv.) (Fig. 2a), indicating the 2:1 binding ratio of **Z** with Al^{3+}. Plotting of the fluorescence intensity at 496 nm versus the concentration of Al^{3+} (0-3 μM) showed a good linear relationship (R^2 = 0.99636) (Fig. S4). Moreover, a significant red-shift with two isobestic points at 356 and 388 nm was observed upon the gradual addition of Al^{3+} (Fig. 2b), and the absorbance intensity ratios of **Z** at 427 nm and 367 nm (A_{427} /A_{367}) increased linearly with the amount of Al^{3+} ranging from 1.2 μM to 3.2 μM (Fig. S5), showing a clear ratiometric absorbance response of the probe **Z** towards Al^{3+}. The detection limits of probe **Z** for Al^{3+} were found as low as 4.08×10^{-8} M and 8.47×10^{-9} M for fluorescence and absorbance-ratiometric detection, respectively, both of which were quite lower than the requirement (maximum contaminant is 7.4 μM) of the U.S. Environmental Protection Agency (EPA). This result showed that probe **Z** had high sensitivity towards Al^{3+} ion, and was qualified in the detection of Al^{3+} in drinking water.

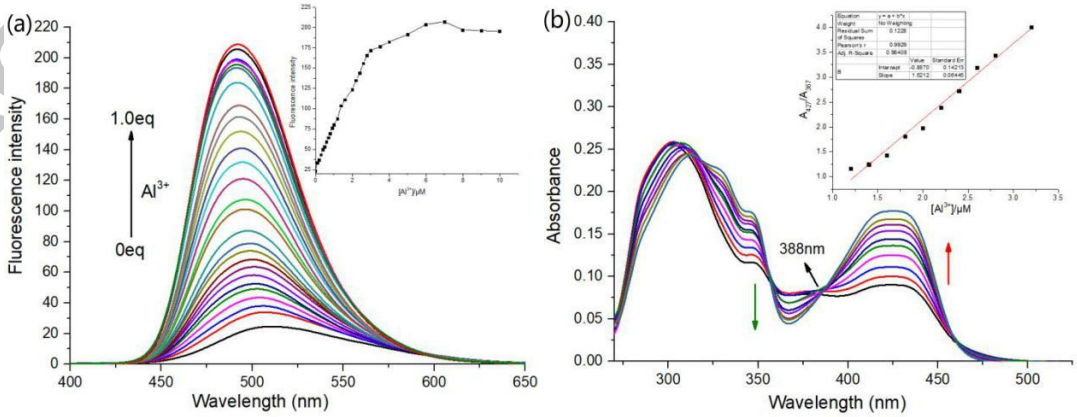

Fig. 2. (a) Fluorescence spectra of **Z** (10 μM) on addition of different amount of Al^{3+} in DMF/H_2O (1/9, v/v, pH = 7.4, 0.01 M HEPES). Inset: fluorescence intensity at 496 nm versus the number of equiv. of Al^{3+} added. (b) UV–vis absorption spectra of **Z** (10 μM) in DMF/H_2O (1/9, v/v, pH = 7.4, 0.01 M HEPES) upon the addition of

Al^{3+} (1.2-3.2 μM). Inset: absorbance intensity at 427 nm/367 nm as a function of Al^{3+} (0.12–0.32 equiv.) in DMF/H2O(1/9, v/v, pH = 7.4, 0.01 M HEPES).

To further confirm the 2:1 stoichiometry between **Z** and Al^{3+}, Job's plot analysis was performed in DMF/H_2O (1/9, v/v, pH = 7.4, 0.01 M HEPES). As show in Fig. 3, the maximum emission intensity of the tested solution was seen when the mole ratio of Al^{3+} appeared at 0.3, indicating the 2:1 binding mode between **Z** and Al^{3+}. This result was further confirmed by a peak at m/z 831.1619, which was assignable to $[2\mathbf{Z} - 2H^{+} + Al^{3+}]^{+}$ (calcd. m/z 831.1640) in the ESI mass spectrum (Fig.4). According to the nonlinear curve fitting of the fluorescence and UV–vis titration data, the binding constants of probe **Z** for Al^{3+} were determined as $2.139\times10^{5}\ M^{-1}$ and $1.556\times10^{5}\ M^{-1}$ (Fig. S6-S7), respectively, based on the Benesi-Hildebrand plot. This result showed the excellent stability of **Z**-Al^{3+} complex.

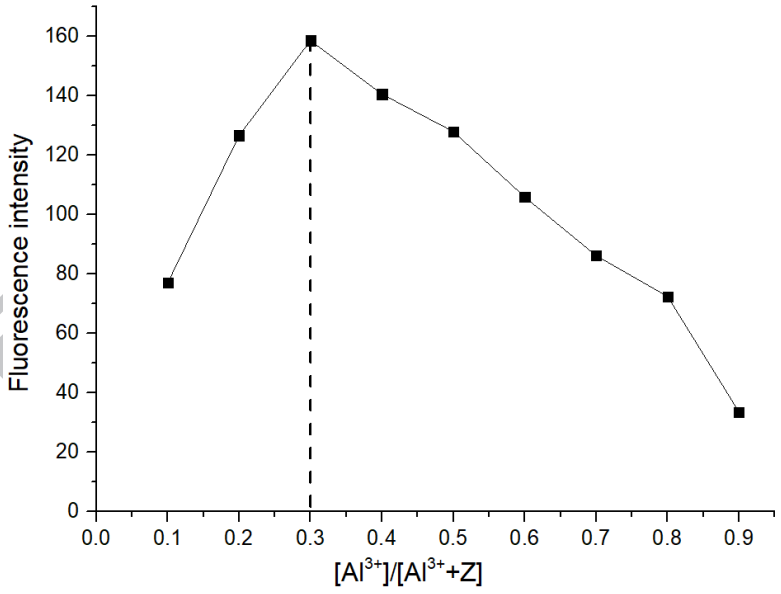

Fig. 3. Job plot of Al^{3+} complex formation. {$[Al^{3+}]/([Al^{3+}] + [\mathbf{Z}])$} is the molar fraction of Al^{3+} ion.

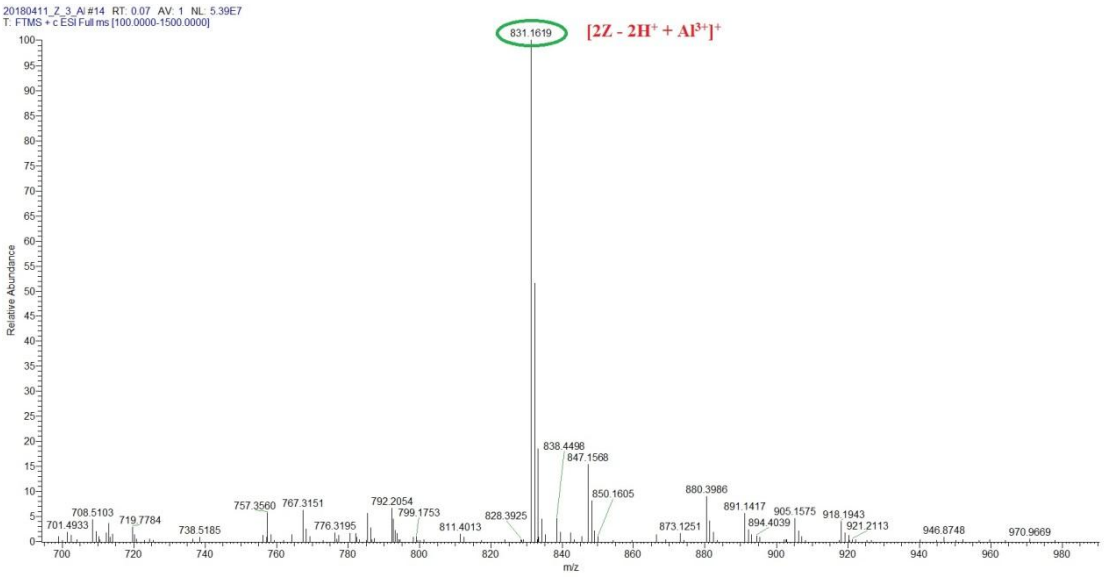

Fig. 4. ESI–MS spectrum of **Z** (50 μM) upon addition of 5 equiv. of Al^{3+} in DMF.

Moreover, the high stability of **Z**-Al^{3+} complex was evaluated through reversibility analysis of **Z** for Al^{3+} in DMF/H_2O (1/9, v/v, pH = 7.4, 0.01 M HEPES). According to recent reports, F^- and $EDTA^{2-}$ had been used to study the reversibility of **Z** for aluminum ions [26, 27], so we conducted the reversibility experiment on the probe **Z** (10 μM) for Al^{3+} (10 μM) mixed with F^- and $EDTA^{2-}$ (10 μM) (Fig. 5), respectively. The absorption and fluorescence spectra of **Z**-Al^{3+} + $EDTA^{2-}$ and **Z**-Al^{3+} + F^- were almost same as that of **Z**-Al^{3+}, respectively, which verified the higher binding constant of **Z**-Al^{3+} complex. The comparative analysis between **Z** and some previously reported sensors were summarized in Table 1.

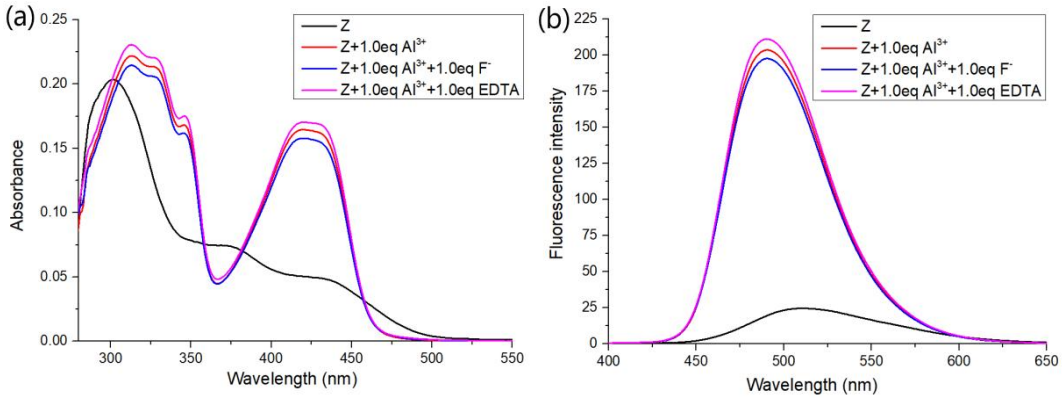

Fig. 5. (a) The absorption properties of the probe Z in response to Al^{3+} (1.0 equiv.) in the presence of F^- and $EDTA^{2-}$ (1.0 equiv.) in DMF/H_2O(1/9, v/v, pH = 7.4, 0.01 M HEPES). (b) Fluorescence spectra of Z in response to Al^{3+} (1.0 equiv.) in the presence of F^- and $EDTA^{2-}$ (1.0 equiv.) in DMF/H_2O (1/9, v/v, pH = 7.4, 0.01 M HEPES).

Table 1. Comparison of different properties of **Z** with recently reported probes used as fluorescent sensor for Al^{3+}.

Ref.	Methods of detection	Detection Medium	LOD	Binding Constants	Recovery	pH range
[28]	Ratiometric fluorescent	CH_3CN/H_2O (1:3)	8×10^{-7} M	4.9×10^{4} M^{-1}	NR	3-10
[29]	Fluorescent	Methanol	9.24×10^{-7} M	9.1×10^{4} M^{-1}	F^-	NR
[30]	Colorimetric and fluorescent	Ethanol/H_2O (3:1)	3.48×10^{-8} M	1.3×10^{4} M^{-1}	$EDTA^{2-}$	5-11
[31]	Fluorescent	Ethanol	2.72×10^{-9} M	5.06×10^{4} M^{-1}	$EDTA^{2-}$	NR
[32]	Fluorescent	Tris-HCl aqueous buffer (0.2% methanol, pH=7.0)	9.2×10^{-8} M	NR	F^-	NR
[33]	Fluorescent	DMSO/H_2O (1:5) HEPES pH = 7.2	1.05×10^{-8} M	8.5×10^{5} M^{-1}	F^-	4-10
[34]	Fluorescent	CH_3CN	3.1×10^{-7} M	5.44×10^{4} M^{-1}	NR	NR
[35]	Fluorescent	Methanol	1.59×10^{-7} M	6.37×10^{4} M^{-1}	$EDTA^{2-}$	NR
[36]	Fluorescent	DMF/H_2O (9:1)	6.7×10^{-6} M	3.21×10^{6} M^{-1}	$EDTA^{2-}$	5-13
This work	Ratiometric absorbance fluorescent	DMF/H_2O (1:9) HEPES pH = 7.4	8.47×10^{-9} M[a] 4.08×10^{-8} M[b]	1.556×10^{5} M^{-1} 2.139×10^{5} M^{-1}	None of $EDTA^{2-}$ and F^-	4-10

LOD: The limit of detection; NR: Not reported in the corresponding paper.

In order to determine the selectivity of the probe **Z** to aluminum ions in the presence of other cations, we also conducted the competitive experiment on the probe **Z** (10 μM) for Al^{3+} (50 μM) mixed with other tested metal ions (Na^+, K^+, Mg^{2+}, Ca^{2+}, Ba^{2+}, Cr^{3+}, Mn^{2+}, Co^{2+}, Ni^{2+}, Cu^{2+}, Zn^{2+}, Cd^{2+}, Hg^{2+} and Pb^{2+}) (50 μM) (Fig. 6).The fluorescence intensity of **Z**-Al^{3+} complexation was almost unaffected except for Co^{2+}, Ni^+, and Cu^{2+}, which could inhibit the emission intensity (496 nm) to different extent. Although Co^{2+}, Ni^{2+} had interference on the detection of Al^{3+}, the fluorescence intensity was still strong enough for the Al^{3+}detection. The existence of Cu^{2+} almost quenched the fluorescence intensity due to its paramagnetic effect. Hence, **Z** has its limitation in that it can detect Al^{3+} in the presence of most metal ion except Cu^{2+}.

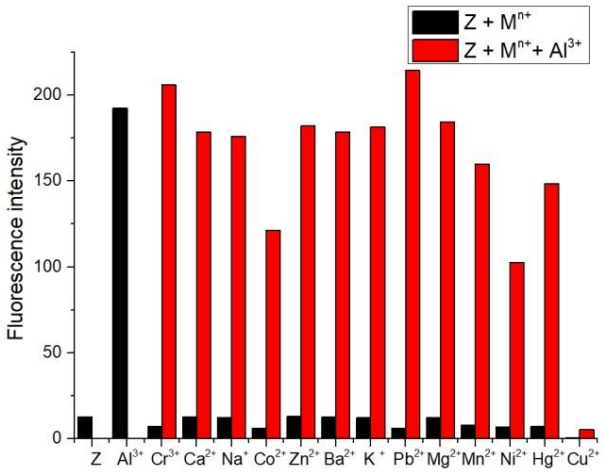

Fig. 6. Competition experiment of **Z** toward Al^{3+} in the presence of 5 equiv. of other cations. [**Z**] = 10 μM, [Al^{3+}] = 50 μM, and [X^{n+}] = 50 μM in DMF/H_2O (1/9, v/v, pH = 7.4, 0.01 M HEPES). λ_{ex} = 350 nm.

3.2. Binding mode and sensing mechanism

The FT-IR spectra of **Z** and **Z**-Al^{3+} complexes were measured (Fig. 7), respectively. Compared with the FT-IR spectra of **Z,** the OH absorption at 3409 cm^{-1} vanished and the C-O of phenolic hydroxyl shifted from 1278 cm^{-1} to 1373 cm^{-1} in the FT-IR spectra of **Z**-Al^{3+} complexes, indicated the deprotonation of phenolic hydroxyl and the coordination of oxygen atom with the Al^{3+} ion. Moreover, the typical imide absorption of -C=N- shifted from 1595 cm^{-1} to 1542 cm^{-1}, which could be caused by the coordination of the imide N atom to the Al^{3+} ions according to previous reports [37].

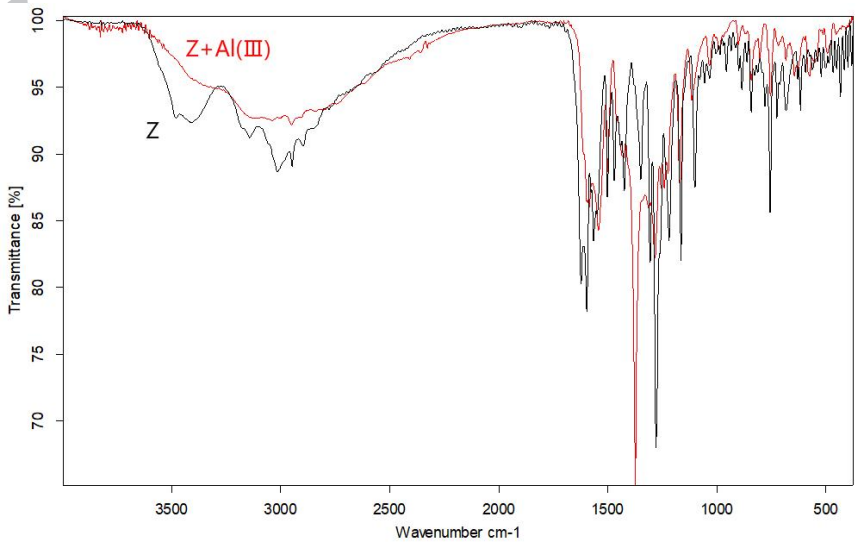

Fig. 7. FT-IR spectra of Z and Z-Al^{3+} complex.

The ^{1}H NMR experiments in the absence and presence of Al^{3+} were carried out in DMSO-d_6 to understand the exact binding mode of **Z**-Al^{3+}. As show in Fig. 8, the proton signal of phenolic hydroxyl (H_a) at 13.42 ppm disappeared, indicating that the oxygen atom of phenolic hydroxyl (a) of **Z** was involved in the coordination to Al^{3+}. The proton signal of amide (H_c) disappeared gradually and a new signal of amide ($H_{c'}$) appeared at 9.25 ppm, indicating the isomerization from (***E***)-configuration to (***Z***)-configuration upon the coordination of nitrogen atom of amide with Al^{3+}.

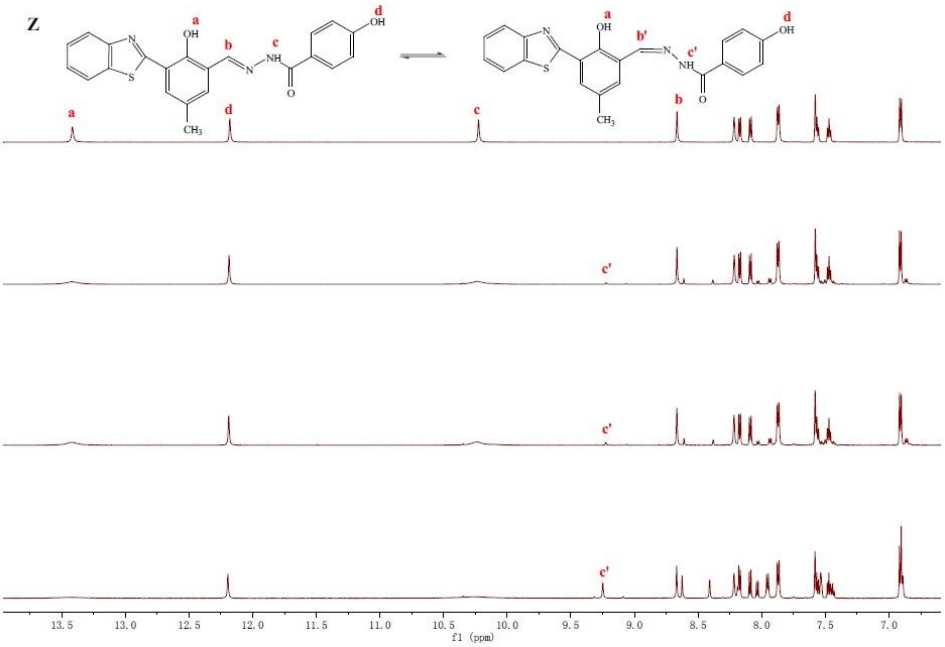

Fig. 8. ^{1}H NMR spectra of Z with Al^{3+} in DMSO-d_6.

According to the analysis of Job's plot, FT–IR spectra, ESI–MS and ^{1}H NMR, a rational bonding mode of **Z** for Al^{3+} was proposed (Scheme 3).

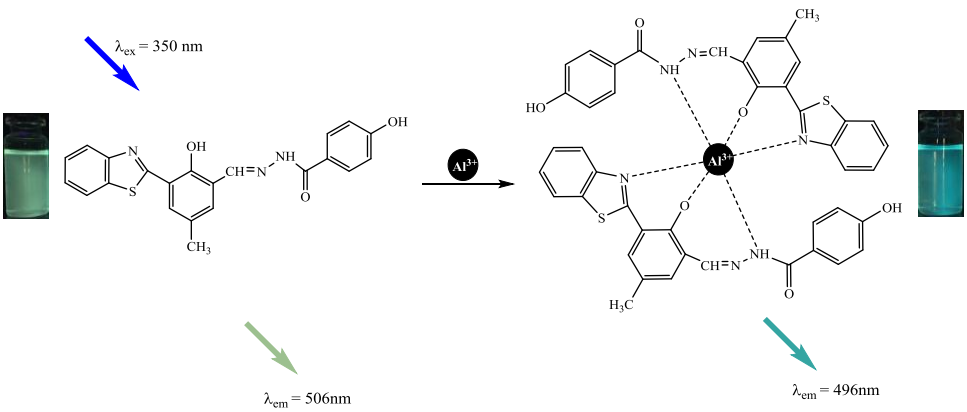

Scheme 3. Probable binding mode of sensor **Z** with Al^{3+} ions.

3.3. Effect of pH on the fluorescence intensity

In order to get a good view in the practical applicability of the probe **Z**, the effect of pH on the fluorescence spectrum of **Z** in the absence and presence of Al^{3+} were measured, respectively. As show in Fig. 9a, the probe **Z** showed a weak fluorescence at 496 nm at pH 7.0, when the pH was changed from 8 to 10, the fluorescence spectrum was red-shift accompanied with the increased intensity centered at 514 nm. The drastic enhancement in emission intensity of **Z** in basic environment was attributed to the deprotonation of phenolic hydroxyl, resulting in the inhibition of ESIPT processes which had been explained in scheme 2. However, when the pH was changed from 6 to 2, the fluorescence maximum emission peak was shifted to 551 nm, and the fluorescence intensity increased gradually. The red-shift in the acidic environment might be attributed to the enhancement of the electron-withdrawing ability of the benzothiazol group upon binding the H^+, thereby enhancing the ICT process upon photoexcitation [38, 39] (Scheme S1).

Furthermore, as show in Fig. 9b, the fluorescence intensity of **Z** almost did not change at 551 nm in the range of pH 2-3 upon the addition of Al^{3+}. However, significant changes in the fluorescence spectrum and fluorescent intensity were observed whatever in acidic or alkaline condition (ranging from the pH 4 to pH 10) compared with **Z** itself in correspondence pH condition. These results showed that probe **Z** could be used as a distinguished probe for Al^{3+} detection in a wide range from acidic (pH 4) to alkaline (pH 10) medium. Taking above results into consideration, the most suitable of pH range for the detection of Al^{3+} was from 4 to 10, based on the result of fluorescence intensity at 496 nm as recorded signal at different pH range from 2 to12 (Fig.S8).

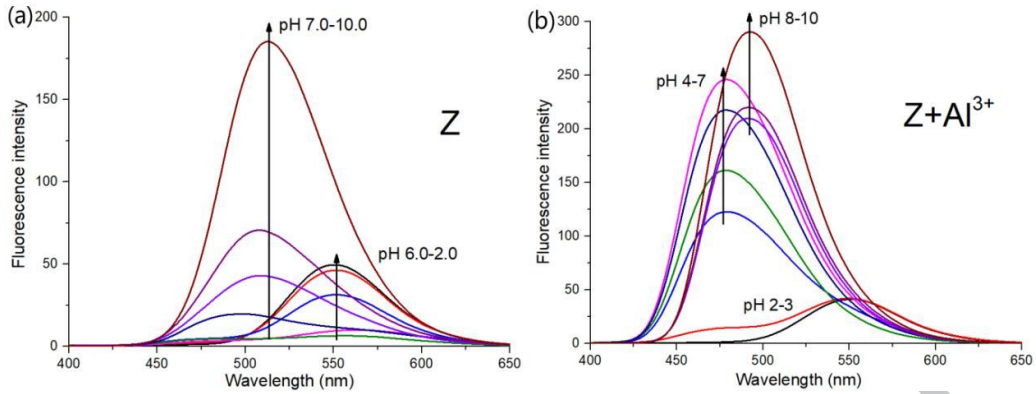

Fig. 9. (a) Plot showing the influence of **Z** (10 μM) in DMF/H_2O (1:9, v/v) with pH; (b) plot showing the influence of solution Z (10 μM)-Al^{3+} (50 μM) in DMF/H_2O (1:9, v/v) at different pH medium.

4. Analytical application

4.1. Application of **Z** for Al^{3+} analysis in water samples

In order to further explore the practical application of **Z**, experimental verification was employed to detect aluminum ions in tap water and pure water. The accuracy was investigated by adding a known amount of standard Al^{3+} to the samples (Table 2). The results showed that probe **Z** had good recoverability and high accuracy for the practical application of aluminum ions in water, which was of great practical value for the detection of Al^{3+} in environmental analysis.

Table 2. Determination of Al^{3+} in water samples from different water sources by standard-addition method (n = 3).

Water samples studied	Amount of standard Al^{3+} added (μmol/L)	Total Al^{3+} found (n=3) (μmol/L)	Recovery of Al^{3+} (n=3) added (%)	RSD (%)	Relative error (%)
ultrapure water	0.200	0.203	101.50	1.06	1.50
	0.400	0.406	101.50	1.16	1.50
Tap water (Department of Chemistry)	0.200	0.193	96.50	1.18	-3.50
	0.400	0.405	101.25	1.44	1.25

4.2. Application in Test Paper

Considering **Z** has good selectivity to Al^{3+}, the colormetric experiments of probe **Z** for Al^{3+} on test paper were examined (Fig. 10). Test papers were emerged in the solution of **Z** mixed with different concentrations of Al^{3+} (0-3 μM) and then dried in air. With increased concentration of Al^{3+}, the test paper displayed a visible color change from light yellow to brilliant cyan, facilitating in the "naked-eye" detection of Al^{3+} under UV light of 365 nm. Hence, this interesting result showed that such test papers had potential application in the fast detection the existence of Al^{3+} in a certain system.

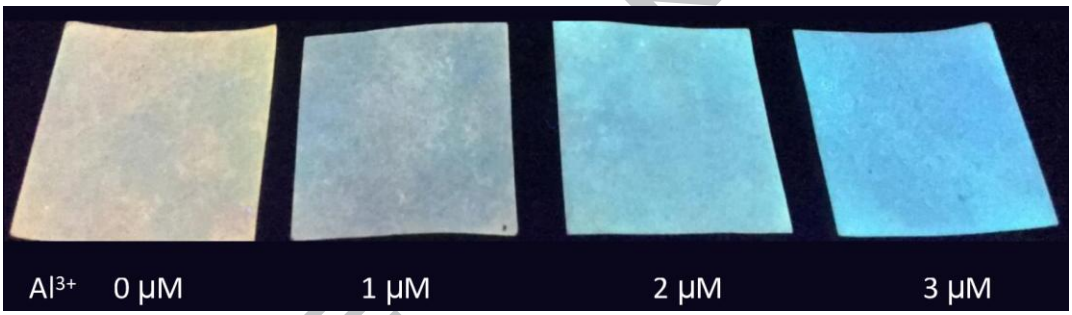

Fig. 10. The photographs of probe **Z** on test strips with different concentrations of Al^{3+} at room temperature under 365 nm UV light.

4.3. Application in CIE diagram

For better understand the trace of the fluorescence changes of the probe **Z** with addition of aluminum ions, the CIE chromaticity coordinates were also calculated from the emission spectrum [40]. The CIE system is a two-dimensional space (XY plane), each point on the chromaticity diagram represents a certain color (Fig. S9). The CIE chromaticity coordinates of **Z** was found to be x=0.2579, y=0.5294 at room temperature. Upon the addition of Al^{3+} (0-3 μM) to the solution of **Z**, the CIE chromaticity coordinates of **Z**-Al^{3+} complex was finally found to be x=0.1441, y=0.4183 when the aluminum ions concentration was 3 μM. This result indicates that the color coordinates shifts gradually from chartreuse to cyan color region upon progressive addition of Al^{3+}

into the solution of **Z**, which is also consistent with the result of the test paper experiment.

4.4. Cells imaging

For evaluation of the potential of detecting Al^{3+} in cells with **Z**, the human stromal cell (HSC), this endometrium fibroblast cell line was derived from the human stromal cells and immortalized with hTERT, has been used as an *in vetro* model. As determined by laser confocal microscope (λ_{ex}= 405 nm, λ_{em}= 490 nm) (Fig. 11 A), the cells incubated with 0 μM of Al^{3+} and 0.1 mM of **Z** for 2 hours did not give any intracellular fluorescence. When cells were incubated with 5 μM of Al^{3+} and 0.1 mM of **Z** for 2 hours, weak fluorescence was observed (Fig. 11 B). After cells were incubated with 50 μM of Al^{3+} and 0.1 mM of **Z** for 2 hours, strong fluorescence appeared (Fig. 11 C). These results suggest that the probe **Z** have potential bio-medical applications.

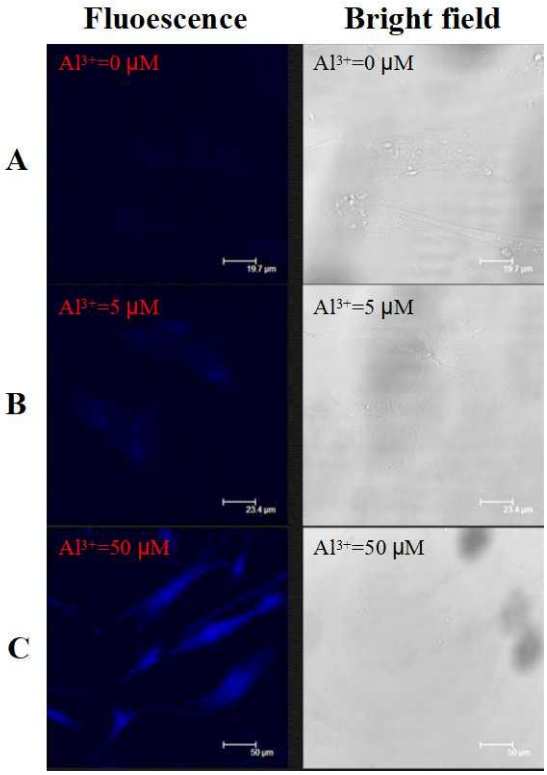

Fig. 11. (A) The cells was incubated 2 hours with **Z** (0.1 mM); (B) cells was incubated 5 μM of Al^{3+} and 0.1 mM of **Z**; (C) cells was incubated 50 μM of Al^{3+} and 0.1 mM of **Z**.

5. Conclusions

In conclution, chemosensor **Z** with benzothiazole fluorophore was synthesized and employed in the detection of Al^{3+} ions based on the combination mechanism of CHEF and ESIPT processes. **Z** exhibited fluorescence turn-on and ratiometric absorbance detection of Al^{3+} ions. A 2:1 binding mode of **Z** and Al^{3+} was confirmed by job's plot and HRMS, and the detection limit (8.47 nM) was qualified in the detection of Al^{3+} in drinking water. Moreover, **Z** was achieved in fast determination the existence of Al^{3+} by filter paper, and cell imaging in human stromal cell (HSC).

Acknowledgements

This work was supported by the Postdoctoral Scientific Research Developmental Fund of Heilongjiang Province (No. LBH-Q14023).

Appendix A. Supporting information

Supplementary data associated with this article can be found in the online version at

References

[1] Q. P. Diao, P. Y. Ma, L. L. Lv, T. C. Li, Y. Sun, X. H. Wang, D. Q. Song, A water-soluble and reversible fluorescent probe for Al^{3+} and F^- in living cells, Sens. Actuators B: Chem. 229 (2016) 138-144.

[2] B. Sen, S. K. Sheet, R. Thounaojam, R. Jamatia, A. K. Pal, K. Aguan, S. Khatua, A coumarin based Schiff base probe for selective fluorescence detection of Al^{3+} and its application in live cell imaging. Spectrochim. Acta Part A 173 (2017) 537–543.

[3] U. Panda, S. Roy, D. Mallick, A. Layek, P. P. Ray, C. Sinha, Aggregation induced emission enhancement (AIEE) of fluorenyl appended Schiff base : A turn on fluorescent probe for Al^{3+}, and its photovoltaic effect, J. Lumin. 181 (2017) 56–62.

[4] Y. S. Dong, T. Q. Liu, X. J. Wan, H. Pei, L. S. Wu, Y. W. Yao, Facile one-pot synthesis of bipyridine-based dual-channel chemosensor for the highly selective and sensitive detection of aluminum ion, Sens. Actuators B: Chem. 241 (2017) 1139–1144.

[5] P. F. Good, C. W. Olanow, D. P. Perl, Neuromelanin-containing neurons of the substantia nigra accumulate iron and aluminum in Parkinson's disease: a LAMMA study, Brain Res. 593 (1992) 343–346.

[6] G. D. Fasman, Aluminum and Alzheimer's disease: model studies, Coord. Chem. Rev. 149 (1996) 125-165.

[7] M. Kawahara, K. Muramoto, K. Kobayashi, H. Mori, Y. Kuroda, Aluminum Promotes the Aggregation of Alzheimer's Amyloid β-Protein in Vitro, Biochem. Biophys. Res. Commun. 198 (1994) 531–535.

[8] Y. Wang, Z. Y. Ma, D. L. Zhang, J. L. Deng, X. Chen, C. Z. Xie, X. Qiao, Q. Z. Li, J. Y. Xu, Highly selective and sensitive turn-on fluorescent sensor for detection of Al^{3+} based on quinoline-base Schiff base, Spectrochim. Acta, Part A 195 (2018) 157–164.

[9] D. L. Godbold, E. Fritz, A. Hüttermann, Aluminum toxicity and forest decline, Proc. Natl. Acad. Sci. U. S. A. 85 (1988) 3888–3892.

[10] H. Sade, B. Meriga, V. Surapu, J. Gadi, M. S. L. Sunita, P. Suravajhala, P. B. K. Kishor, Toxicity and tolerance of aluminum in plants: tailoring plants to suit to acid soils, Biometals, 29 (2016) 187–210.

[11] J. Barceló, C. Poschenrieder, Fast root growth responses, root exudates, and internal detoxification as clues to the mechanisms of aluminium toxicity and resistance: a review. Environ. Exp. Bot. 48 (2002) 75–92.

[12] Z. Huang, S. Ding, D. Yu, F. Huang. G. Feng, Aldehyde group assisted thiolysis of dinitrophenyl ether: a new promising approach for efficient hydrogen sulfide probes, Chem. Commun. 50 (2014) 9185–9187.

[13] C. Y. Yang, Y. Chen, K. Wu, T. Wei, J. L. Wang, S. S. Zhang, Y. F. Han, A reactive probe for Cu^{2+} based on the ESIPT mechanism and its application in live-cell imaging, Anal. Methods, 7 (2015) 3327–3330.

[14] B. Gu, Y. Chen, L. Y. Huang, W. Su, X. L. Duan, H. T. Li, S. Z. Yao, A benzothiazole-based fluorescent probe for distinguishing and bioimaging of Hg^{2+} and Cu^{2+}, Anal. Chim. Acta 954 (2017) 97-104.

[15] D. Maity, T. Govindaraju, Conformationally Constrained (Coumarin-Triazolyl-Bipyridyl) Click Fluoroionophore as a Selective Al^{3+} Sensor, Inorg. Chem. 49 (2010) 7229-7231.

[16] C. S. Liang, W. H. Bu, C. L. Li, G. W. Men, M. Y. Deng, Y. K. Jiangyao, H. C. Sun, S. M. Jiang, A highly selective fluorescent sensor for Al3+ and the use of the resulting complex as a secondary sensor for PPi in aqueous media: its applicability in live cell imaging, Dalton Trans. 44 (2015) 11352-11359.

[17] W. H. Wang, Z. F. Mao, M. D. Wang, L. J. Liu, D. W. J. Kwong, C. H. Leung, D. L. Ma, A long lifetime luminescent iridium(III) complex chemosensor for selective switch-on detection of Al^{3+} ions, Chem. Commun. 52 (2016) 3611–3614.

[18] C. C. Chang, F. Wang, J. Qiang, Z. J. Zhang, Y. H. Chen, W. Zhang, Y. Wang, X. Q. Chen,

Benzothiazole-based fluorescent sensor for hypochlorite detection and its application for biological imaging, Sens. Actuators B: Chem. 243 (2016) 22–28.

[19] L. J. Tang, X. Dai, X. Wen, D. Wu, Q. Zhang, A rhodamine–benzothiazole conjugated sensor for colorimetric, ratiometric and sequential recognition of copper (II) and sulfide in aqueous media, Spectrochim. Acta, Part A 139 (2015) 329–334.

[20] E. T. Feng, R. M. Lu, C. B. Fan, C. H. Zheng, S. Z. Pu, A fluorescent sensor for Al^{3+} based on a photochromic diarylethene with a hydrazinobenzothiazole Schiff base unit, Tetrahedron Lett. 58 (2017) 1390–1394.

[21] E. T. Feng, C. B. Fan, N. S. Wang, G. Liu, S. Z. Pu, A highly selective diarylethene chemosensor for colorimetric detection of CN^- and fluorescent relay-detection of Al^{3+} /Cr^{3+}, Dyes Pigm. 151 (2018) 22–27.

[22] S. Y. Li, D. B. Zhang, J. Y. Wang, R. M. Lu, C. H. Zheng, S. Z. Pu, A novel diarylethene-hydrazinopyridine-based probe for fluorescent detection of aluminum ion and naked-eye detection of hydroxide ion, Sens. Actuators B: Chem. 245 (2017) 263–272.

[23] L. J. Tang, S. L. Ding, K. L. Zhong, S. H. Hou, Y. J. Bian, X. M. Yan, A new 2-(2′-hydroxyphenyl)quinazolin-4(3H)-one derived acylhydrazone for fluorescence recognition of Al^{3+}, Spectrochim. Acta, Part A 174 (2017) 70–74.

[24] Z. Liao, Y. Liu, S. F. Han, D. Wang, J. Q. Zheng, X. J. Zheng, L. P. Jin, A novel acylhydrazone-based derivative as dual-mode chemosensor for Al^{3+}, $Zn^{2+}$and Fe^{3+} and its applications in cell imaging, Sens. Actuators B: Chem. 244 (2017) 914–921.

[25] S. B. Roy, K. K. Rajak, A quinoline appended naphthalene derivative based AIE active“turn–on” fluorescent probe for the selective recognition of Al^{3+} and colourimetric

sensor for Cu^{2+} : Experimental and computational studies, J. Photochem. Photobiol. A: Chem. 332 (2017) 505–514.

[26] A. Roy, S. Dey, P. Roy, A ratiometric chemosensor for Al^{3+} based on naphthalene-quinoline Conjugate with the resultant complex as secondary sensor for F^{-}: Interpretation of molecular logic gates, Sens. Actuators B: Chem. 237 (2016) 628–642.

[27] F. Yu, L. J. Hou, L. Y. Qin, J. B. Chao, Y. Wang, W. J. Jin, A new colorimetric and turn-on fluorescent chemosensor for Al^{3+} in aqueous medium and its application in live-cell imaging, J. Photochem. Photobiol. A: Chem. 315 (2016) 8–13.

[28] D. J. Wang, X. P. Fan, S. G. Sun, S. Z. Du, H. J. Li, J. L. Zhu, Y. F. Tang, M. X. Chang, Y. Q. Xu, Substituent effect: A new strategy to construct a ratiometric fluorescent probe for detection of Al^{3+} and imaging in vivo, Sens. Actuators B: Chem. 264 (2018) 304–311.

[29] C. Lim, H. Seo, J. H. Choi, K. S. Kim, A. Helal, H. S. Kim, Highly selective fluorescent probe for switch-on Al^{3+} detection and switch-off F^{-} detection, J. Photochem. Photobiol. A: Chem. 356 (2018) 312–320.

[30] B. J. Pang, C. R. Li, Z. Y. Yang, Design of a colorimetric and turn-on fluorescent probe for the detection of Al(III), J. Photochem. Photobiol. A: Chem. 356 (2018) 159–165.

[31] X. L. Yue, Z. Q. Wang, C. R. Li, Z. Y. Yang, A highly selective and sensitive fluorescent chemosensor and its application for rapid on-site detection of Al^{3+}, Spectrochim. Acta, Part A 193 (2018) 415–421.

[32] Q. P. Diao, P. Y. Ma, L. L. Lv, T. C. Li, Y. Sun, X. H. Wang, D. Q. Song, A water-soluble and reversible fluorescent probe for Al^{3+} and F^{-} in living cells, Sens. Actuators B: Chem. 229 (2016) 138–144.

[33] D. Sarkar, P. Ghosh, S. Gharami, T. K. Mondal, N. Murmu, A novel coumarin based molecular switch for the sequential detection of Al^{3+} and F^{-}: Application in lung cancer live cell imaging and construction of logic gate, Sens. Actuators B: Chem. 242 (2017) 338–346.

[34] M. Tajbakhsh, G. B. Chalmardi, A. Bekhradnia, R. Hosseinzadeh, N. Hasani, M. A. Amiri, A new fluorene-based Schiff-base as fluorescent chemosensor for selective detection of Cr^{3+} and Al^{3+}, Spectrochim. Acta, Part A 189 (2018) 22–31.

[35] N. N. Li, S. Zeng, M. Q. Li, Y. Q. Ma, X. J. Sun, Z. Y. Xing, J. L. Li, A Highly Selective Naphthalimide-Based Chemosensor: "Naked-Eye" Colorimetric and Fluorescent Turn-On Recognition of Al^{3+} and Its Application in Practical Samples, Test Paper and Logic Gate, J. Fluoresc. 28 (2018) 347–357.

[36] S. M. Hossain, K. Singh, A. Lakma, R. N. Pradhan, A. K. Singh, A schiff base ligand of coumarin derivative as an ICT-Based fluorescence chemosensor for Al^{3+}, Sens. Actuators B: Chem. 239 (2017) 1109–1117.

[37] H. Y. Liu, B. B. Zhang, C. Y. Tan, F. Liu, J. K. Cao, Y. Tan, Y. Y. Jiang, Simultaneous bioimaging recognition of Al^{3+} and Cu^{2+} in living-cell, and further detection of $F^{-}$and S^{2-} by a simple fluorogenic benzimidazole-based chemosensor, Talanta 161 (2016) 309–319.

[38] W. F. Niu, Z. W. Wei, J. Jia, S. M. Shuang, C. Dong, K. M. Yun, A ratiometric emission NIR-fluorescent probe for sensing and imaging pH changes in live cells, Dyes Pigm. 152 (2018) 155–160.

[39] M. T. Sun, L. B. Du, H. Yu, K. Zhang, Y. Liu, S. H. Wang, An intramolecular charge transfer process based fluorescent probe for monitoring subtle pH fluctuation in living cells, Talanta 162 (2017) 180–186.

[40] M. Kumar, A. Kumar, M. S. H. Faizi, S. Kumar, M. K. Singh, S. K. Sahu, S. Kishor, R. P. John, A selective 'turn-on' fluorescent chemosensor for detection of Al^{3+} in aqueous medium: Experimental and theoretical studies, Sens. Actuators B: Chem. 260 (2018) 888–899.

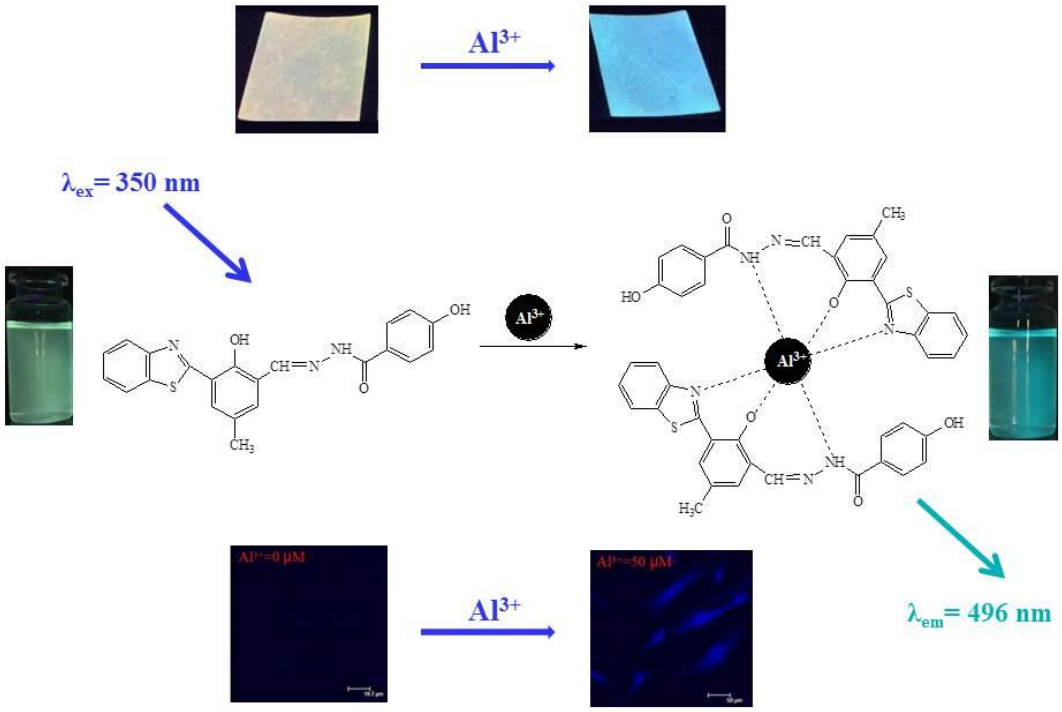

Highlights

- Chemosensor **Z** with benzothiazole fluorophore was synthesized and characterized.
- Chemosensor **Z** indeed exhibits highly selective fluorescence responses to Al^{3+} with a 9-fold fluorescence enhancement and ratiometric absorption detection
- The limit of detection (LOD) for Al^{3+} was 4.08×10^{-8} M and 8.47×10^{-9} M for fluorescence and absorbance-ratiometric detection, respectively.
- **Z** was successfully applied to form paper strip sensor for Al^{3+} and cell imaging in HSC.